Hindawi Publishing Corporation
Journal of Nanomaterials
Volume 2014, Article ID 190529, 11 pages
http://dx.doi.org/10.1155/2014/190529

Research Article

Solvothermal Synthesis of Mn_3O_4 Nanoparticle/Graphene Sheet Composites and Their Supercapacitive Properties

Y. F. Liu,[1,2] G. H. Yuan,[1] Z. H. Jiang,[1] and Z. P. Yao[1]

[1] *School of Chemical Engineering and Technology, Harbin Institute of Technology, Harbin 150001, China*
[2] *College of Environmental and Chemical Engineering, Heilongjiang University of Science and Technology, Harbin 150022, China*

Correspondence should be addressed to G. H. Yuan; yunfu33@126.com and Z. H. Jiang; Jiangzhaohua@hit.edu.cn

Received 25 July 2014; Accepted 10 October 2014; Published 27 October 2014

Academic Editor: Shiren Wang

Mn_3O_4 nanoparticle/graphene sheet (GM) composites were synthesized via a one-pot and low-cost solvothermal process in an ethanol solution. The as-prepared materials were characterized by X-ray diffraction, field emission scanning electron microscopy, and transmission electron microscopy. Results showed that the nanosized Mn_3O_4 particles had tetragonal hausmannite structure and were successfully loaded on the graphene sheets. Moreover, the electrochemical performances of GM composites produced by different mass percents of Mn^{2+}/graphite oxide (GO) were evaluated by means of cyclic voltammetry and galvanostatic charge-discharge studies. The composite prepared with Mn^{2+}/GO mass percent of 10 : 90 showed a high specific capacitance of 245 F/g at 5 mV/s in the 6 M KOH solution and better long-term stability along with 81% of its initial capacitance after 1200 cycles at 0.5 A/g.

1. Introduction

Supercapacitors (SCs) are considered as promising candidates for energy storage due to simple principle, long cyclic life, and quick charging/discharging [1]. Based on their different charge-storage mechanisms, SCs can be classified into the electrochemical double-layer capacitors (EDLCs) and redox capacitors [2]. In contrast to EDLCs, redox capacitors can obtain much higher capacitance values [3], because the faradaic processes occur both on the surface and in the bulk near the surface of the solid electrode. Therefore, considerable effort has been made on the field of redox capacitors.

The electrode materials of redox capacitors usually have two types: metal oxides and conducting polymers, of which the former can exhibit better electrochemical stability than the latter [4]. In general, the metal oxides applied for SCs include RuO_2 [5], IrO_2 [6], MnO_2 [7], Mn_3O_4 [8], Co_3O_4 [9], NiO [10], and MoO [11]. Among them, Mn_3O_4 is seen to be a potential electrode material for SCs owning to its low toxicity, low price, and a very high theoretical capacity [12]. But Mn_3O_4 also has the same defects as other metal oxides for electrode materials like the low surface area, the poor electrical conductivity, and the cycling stability [13]. Hence, many researchers have adopted a supporting strategy, by which Mn_3O_4 can be dispersed over a large area and excellent conductivity of carbon-based materials such as carbon nanotube [14, 15], mesoporous carbon [16], carbon fiber [17], and carbon coating [18]. The introduction of these supports not only ensures high utilization of Mn_3O_4 but also assists electron transfer effectively. Therefore, these composites containing Mn_3O_4 and carbon materials exhibit obviously improved electrochemical performances, compared with the bare Mn_3O_4.

Relative to the above these matrix materials, graphene has displayed more outstanding properties such as a faster electron mobility (≥15,000 $cm^2/V{\cdot}s$) [19] and larger surface area (2675 m^2/g) [20], so there are a variety of synthetic methods applied for preparing Mn_3O_4/graphene composites as the supercapacitor electrode materials, for example, sonochemical method [21], hydrothermal or solvothermal routes [22–24], chemical synthesis method [25], oxidation method [26], atom-economic method [27] and microwave-assisted hydrothermal synthesis route [28], and so forth. In these methods, the solvothermal route requires noncomplex apparatus and simple operation, employed at low temperature (<423 K). The method has also been an effective technique

Table 1: Synthesized conditions and electrochemical performances of Mn_3O_4/graphene composites prepared by hydrothermal or solvothermal routes in published literatures.

Basic synthesis information	Electrolyte	Potential window (V)	Current loador scan rate	Maximum specific capacitance (F/g)	Reference
Graphene sheets + $KMnO_4$ + H_2O + ethylene glycol, solvothermal 393 K for 4 h	1 M Na_2SO_4	−0.3 to 0.7 (Ag/Ag Cl)	5 mV/s	120 (3-electrode)	[22]
GO + $Mn(CH_3COO_2)\cdot 4H_2O$ + ethanol + H_2O, solvothermal 453 K for 11 h	1 M Na_2SO_4	−0.2 to 0.8 (SCE)	5 mV/s	225 (3-electrode)	[23]
GO + $KMnO_4$ + H_2O + hydrazine hydrate, hydrothermal 453 K for 6 h	1 M Na_2SO_4	−0.2 to 0.8 (SCE)	0.1 A/g	171 (3-electrode)	[24]
GO + $Mn(CH_3COO_2)\cdot 4H_2O$ + dimethyl sulfoxide solvothermal 393 K for 24 h	1 M Na_2SO_4	−0.2 to 0.8 (SCE)	0.1 A/g	147 (3-electrode)	[29]

to prepare Mn_3O_4 nanoparticles with controllable size and shape by properly choosing the temperature or reaction time or solvent. The solvents for preparing Mn_3O_4 with solvothermal treatment often are dimethyl sulfoxide [29], methyl alcohol [30], ethylenediamine and ethylene glycol [31], N,N′-dimethylformamide [32], and so forth. In contrast to these solvents, ethanol is becoming a competitive solvent component in the synthesis of Mn_3O_4 nanoparticles and reduction of graphite oxide (GO) to graphene due to its low price and nontoxicity [33].

Table 1 listed the compiled information of Mn_3O_4/graphene composites prepared by hydrothermal or solvothermal routes in currently published literatures. The electrochemical performances of composites changed in a wide range because of their different synthesized conditions. Here we will report an approach to produce Mn_3O_4 nanoparticle/graphene sheet (GM) composites directly from GO and manganese acetate tetrahydrate in the ethanol solution under solvothermal condition. The effects of different mass percent of Mn^{2+}/GO on the electrochemical performances of as-prepared GM composites were investigated. Meantime, the structure and morphology characteristics of GM composites were studied.

2. Experimental

2.1. Solvothermal Synthesis of the GM Composites. GO was synthesized by a modification of the Hummers method [34]. Concentrated H_2SO_4 (70 mL) was added in the mixture of Flake graphite (FG) powder (3.0 g, 25 μm with purity >9.9 wt%) and $NaNO_3$ (1.5 g) in the flask, then cooled on an ice bath, and stirred for 30 min. $KMnO_4$ (9.0 g) was gradually added into the solution and its temperature was controlled under 293 K. After stirring for 2 h in the ice bath, the mixture was transferred into the water bath and kept at 308 K for 1 h. The water (140 mL) was followed to add into the mixture and caused its temperature slowly up to 371 K, maintaining at the temperature for 1 h. Then, the mixture was put into 420 mL warm water (323 K) and treated with 30 mL of 30 wt% H_2O_2. Finally, the solid mixture was separated by the filtration and high-speed centrifugation (8000 Rpm), washed with 5 wt% HCl solution and water, respectively, and dried in vacuum at 323 K for 96 h.

GO (50 mg) was dispersed in ethanol (60 mL) by sonication for 3 h; then the $Mn(CH_3COO)_2\cdot 4H_2O$ powder was added into the solution according to Mn^{2+}/GO mass percent of 5 : 95, 10 : 90, 20 : 80, 30 : 70, 40 : 60, 50 : 50, and 75 : 25, respectively, and continued to ultrasonic dispersal for 1 h. The obtained suspension was sealed into a teflon-lined autoclave (100 mL) and heated at 473 K for 10 h. The last products were filtered, washed with ethanol, and dried in vacuum at 323 K for 24 h. For comparison, pure Mn_3O_4 and graphene sheets (GS) were produced by the above method.

2.2. Materials Characterizations. X-ray diffraction (XRD) patterns of samples were investigated on a Rigaku D/MAX-RB X-ray diffractometer (Cu Kα radiation $\lambda = 0.15406$ nm). X-ray photoelectron spectra (XPS) were obtained with a PHI 5700 ESCA System under Al Kα radiation (1486.6 eV). Raman spectra were recorded by a Jobin Yvon HR800 Raman spectrometer at 458 nm. The morphologies of samples were observed by a field emission scanning electron microscopy (FESEM, Quanta 200F, FEI), transmission electron microscopy (TEM), high resolution transmission electron microscopy (HRTEM), and the corresponding selected area diffraction (SAED) pattern by a Tecnai F20 (FEI) at an accelerating voltage of 200 kV. The element compositions of samples were analyzed by an energy dispersive spectrometer (EDS, EDAX Inc.). Carbon-coated copper grids were used as the sample holders.

2.3. Preparation of Electrodes. The working electrodes were prepared by mixing 80 wt% of as-prepared electrode materials, 10 wt% of carbon black, and 10 wt% of polyvinylidene fluoride as a binder. N-Methyl-pyrrolidone was added to the mixture as the solvent to get homogeneous slurry. Then, the slurry was pasted onto nickel foam current collectors (1 cm^2), followed by drying in vacuum at 373 K for 24 h. Each electrode contained about 8 mg of active material. Activated

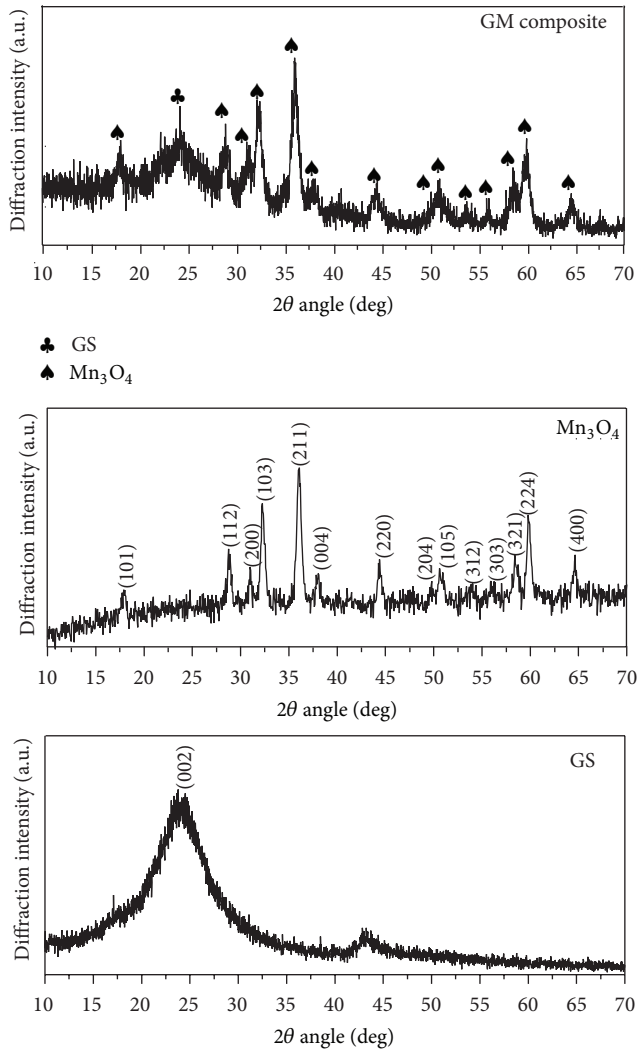

FIGURE 1: XRD patterns of GS, Mn_3O_4, and GM composite prepared with Mn^{2+}/GO mass percent of 50 : 50.

carbon electrodes were prepared as the counter electrode by the above technique.

2.4. Electrochemical Measurements. Supercapacitive properties of as-prepared materials were measured, using three-electrode system with the working electrode, counter electrode, and Hg/HgO electrode as the reference electrode in the 6 M KOH solution at room temperature. CV was investigated on a CHI 604B electrochemical workstation (CHI, Shanghai, China) and GCD curves were tested by a Neware battery testing workstation (Neware, Shenzhen, China).

3. Result and Discussion

3.1. Structures. Figure 1 shows XRD patterns of GS, Mn_3O_4 nanoparticles and GM composite prepared with Mn^{2+}/GO mass percent of 50 : 50. The Bragg (002) peak of GS exhibits a broad peak at 23.67° with d-spacing of 3.58 Å and is larger than the d-spacing (3.36 Å) of FG (2θ = 26.56°), due to forming the disordered layer stacking of GS with a few residual oxygen functional groups [35]. From the XRD pattern of Mn_3O_4 nanoparticles, the peaks of 18.07°, 28.92°, 31.07°, 32.32°, 36.07°, 38.12°, 44.47°, 49.92°, 50.97°, 53.92°, 53.97°, 56.12°, 58.47°, 59.82°, and 72.74° are in good accordance with the standard values of tetragonal hausmannite (JCPDS 24-0734) [36]. It can also be seen that the XRD data of GM composite possess both the (002) peak of GS and the peaks of pure Mn_3O_4. In addition, no peaks corresponding to impurities are found, implying that GM composite produced by solvothermal synthesis is of high purity.

Figure 2(a) displays that the C1s XPS spectrum of GO has an asymmetric photoelectron peak, but the spectrum (Figure 2(b)) of GM composite prepared with Mn^{2+}/GO mass percent of 50 : 50 has only single peak. The C1s peaks of GO and GM composite can be further deconvoluted in four peaks assigned to carbon atoms in different functional groups: C–C/C=C in aromatic rings (~284.6 eV), C–O

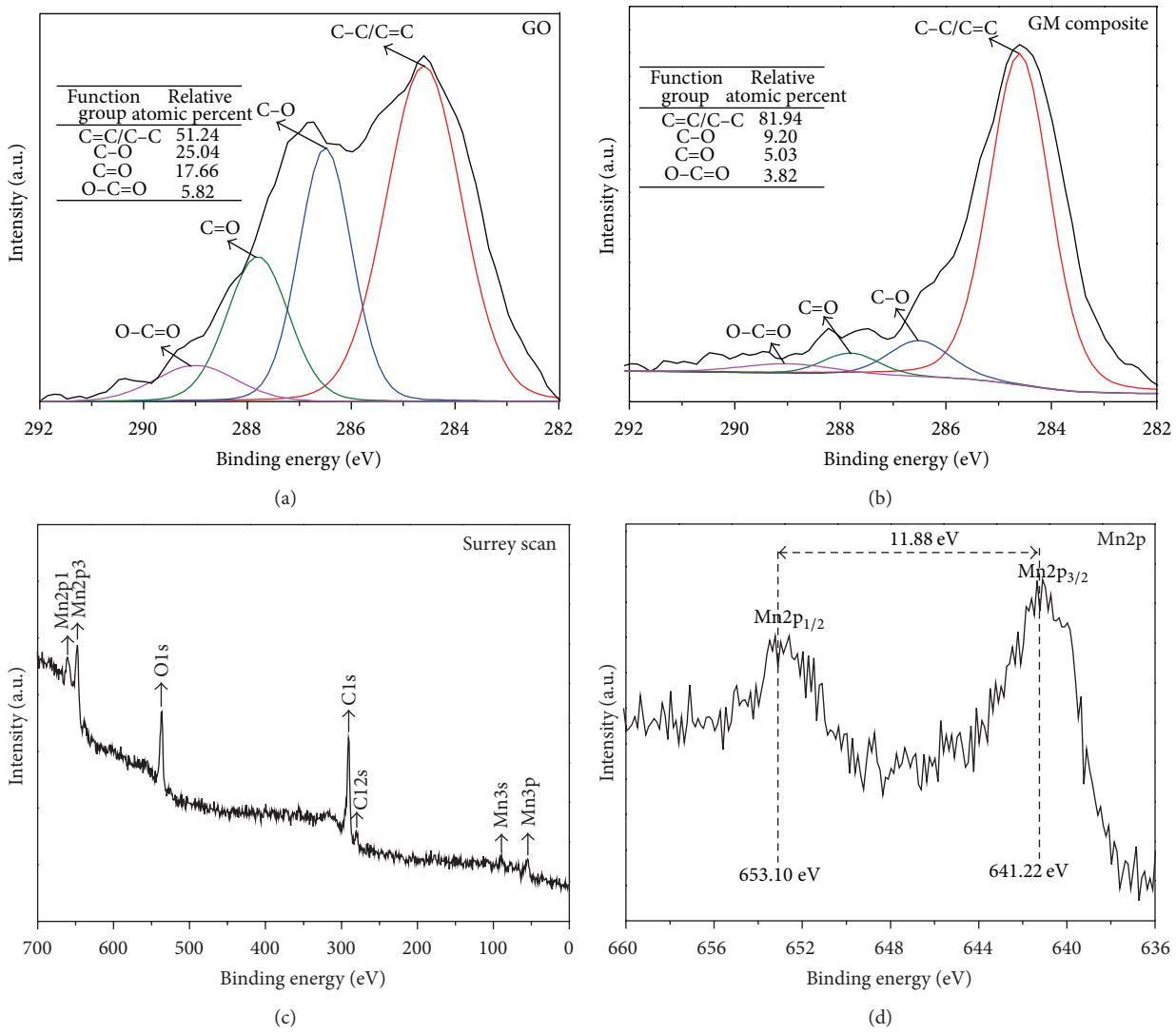

FIGURE 2: XPS spectra of (a) C1s region of GO and (b) C1s region, (c) survey scan, and (d) Mn2p region of GM composite prepared with Mn^{2+}/GO mass percent of 50 : 50.

(hydroxyl and epoxy, ~286.5 eV), C=O (carbonyl, ~287.8 eV), and O–C=O (carboxyl, ~289.0 eV) [37]. Compared with these peaks of GO, the peak intensities of C–O, C=O, and O–C=O groups of GM composite become smaller, and the C/O atomic ratio increases from 2.96 (GO) to 9.28 (GM composite). This indicates that most oxygen-containing groups of GO can be removed and its π-bonding restored to obtain GS through solvothermal reaction.

The XPS measurement of GM composite was carried out in the survey range (0–1400 eV). The survey spectrum (Figure 4(c)) shows that the energy locations of Mn3s, Mn2p, Mn3p, C1s, C2s, and O1s are matched very well with the values reported in the handbook [38]. In the Mn2p region (Figure 4(d)), the binding energy values of $Mn2p_{3/2}$ and $Mn2p_{1/2}$ are 641.22 and 653.10 eV, respectively. The splitting width of spin orbit is 11.88 eV, approaching the previously reported value of Mn_3O_4 [39]. This exhibits that the solvothermal strategy is an efficient way to prepare GM composite in the ethanol solution.

Raman spectra (Figure 3) show two prominent peaks (D and G bands) of GO at about 1361 and 1594 cm^{-1}, respectively, and a typically sharp peak of Mn_3O_4 at 651 cm^{-1} [40, 41]. The G band corresponds to the first order scattering of the E_{2g} phonon of C sp^2 atoms, while D band is due to a breathing mode of κ-point phonons of A_{1g} symmetry [42]. In the Raman spectroscopy of as-prepared composite, there are three peaks at around 649, 1356, and 1590 cm^{-1}, respectively and its D/G intensity is higher than that of GO. The increased intensity value may be explained that some oxygen atoms are eliminated to generate more defects [43] and a great deal of smaller graphitic domains formed during the reduction of exfoliated GO [44]. These results further testify that GM composite can be obtained with one-pot solvothermal method.

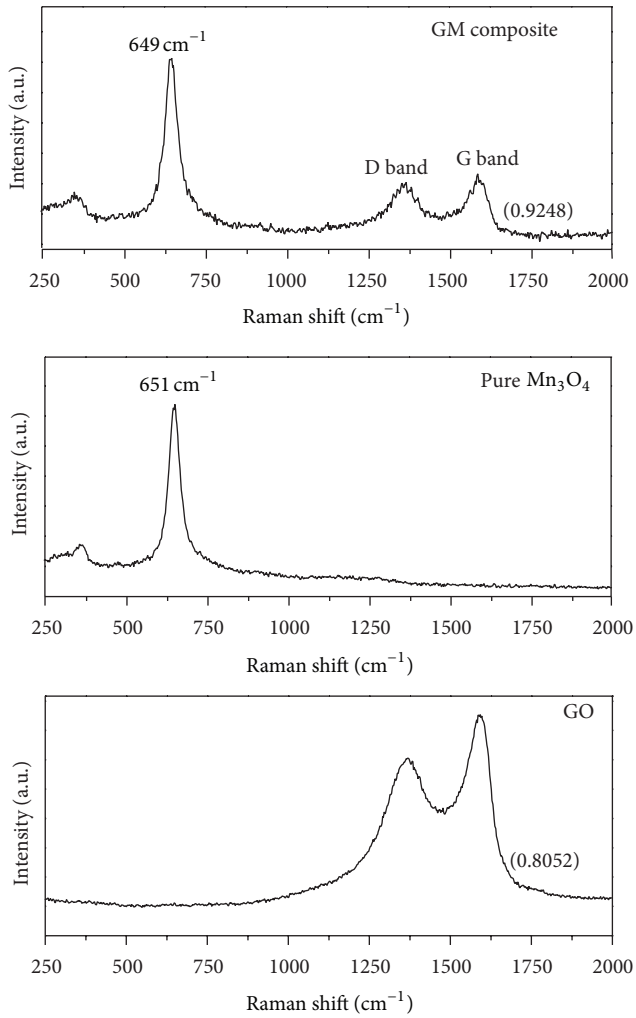

Figure 3: Raman spectra of GO, Mn_3O_4, and GM composite prepared with Mn^{2+}/GO mass percent of 50 : 50. Numbers in the bracket represent the D/G intensity ratio of GO and GM composite.

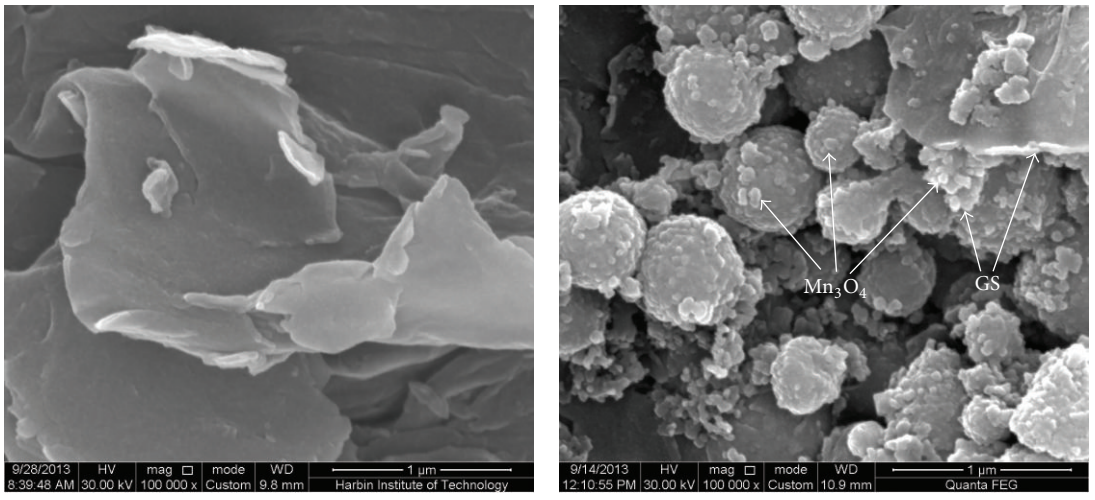

(a) (b)

Figure 4: FESEM images of GS (a) and GM composite (b) prepared with Mn^{2+}/GO mass percent of 50 : 50.

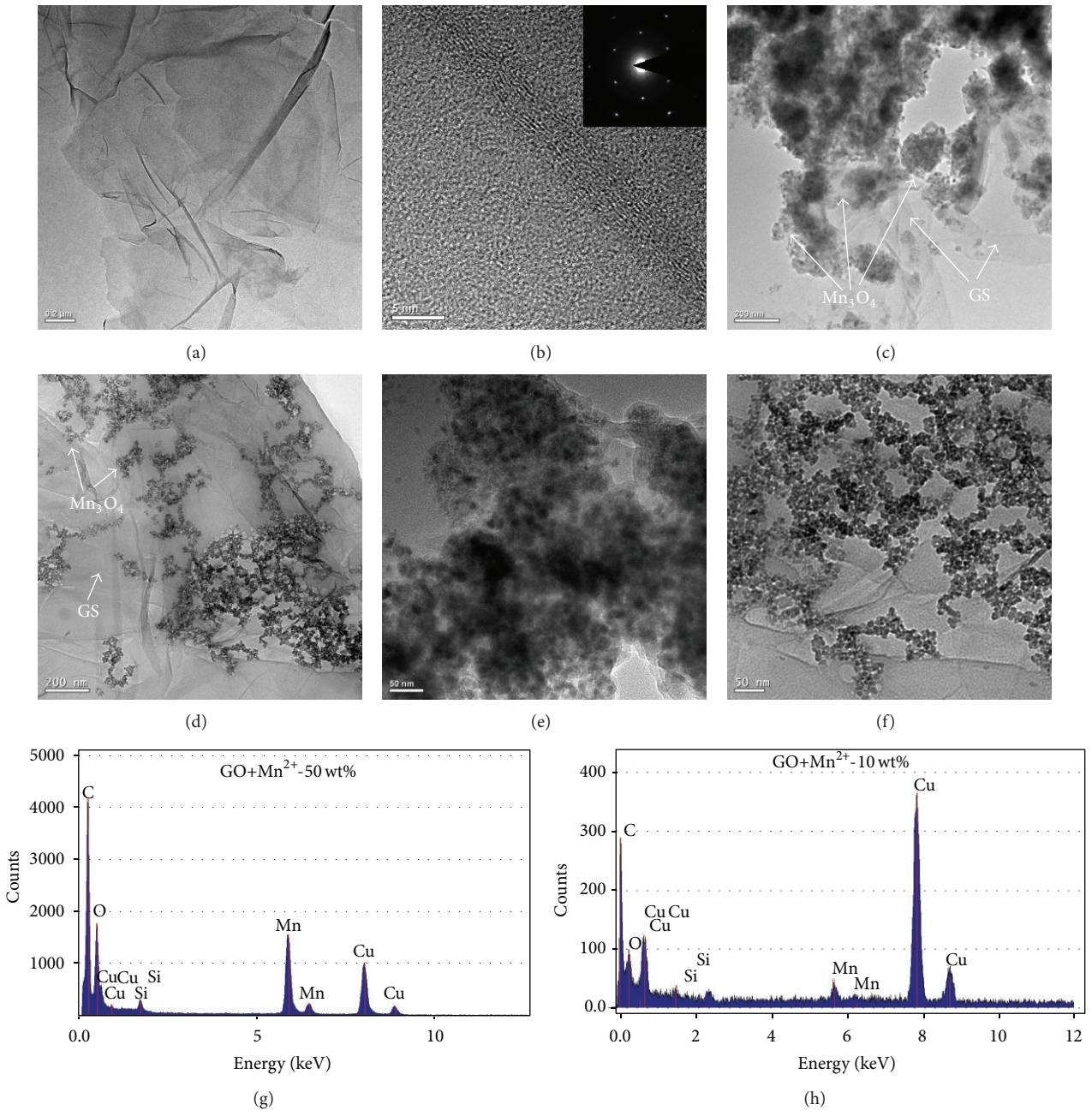

Figure 5: (a) TEM image and (b) HRTEM image of GS. The *inset* is the corresponding SAED pattern. TEM images of GM composite prepared with Mn^{2+}/GO mass percent of 50 : 50 (c, e) and 10 : 90 (d, f). EDS images of GM composites prepared with Mn^{2+}/GO mass percent of 50 : 50 (g) and 10 : 90 (h).

3.2. Morphologies. FESEM images (Figure 4(a)) of GS produced at 473 K by solvothermal synthesis displays an isolated, crumpled, and very thin flake. In addition, Figure 4(b) shows that nanosized Mn_3O_4 particles agglomerating each other are dispersed on the surface of GS. The agglomerated nanoparticles may restrict the electrochemical activity of GM composite.

TEM image (Figure 5(a)) shows that GS at 473 K are a mixture of transparent, curled, few-layer graphene (2–5 layers). The result has also been confirmed by analyzing the folded structure of its edges in the HRTEM image (Figure 5(b)). The corresponding SAED pattern clearly exhibits the typical sixfold symmetry diffraction pattern of a folding graphene layer or two overlapping graphene layers, which is consistent with the result of [45]. TEM image (Figures 5(c) and 5(e)) of GM composite prepared with Mn^{2+}/GO mass percent of 50 : 50 displays the severe agglomeration of Mn_3O_4 nanoparticles loaded on the surface of GS. Then, TEM image (Figures 5(d) and 5(f)) of composite prepared with Mn^{2+}/GO mass percent of 10 : 90 shows Mn_3O_4 nanoparticles are scattered on the surface of GS,

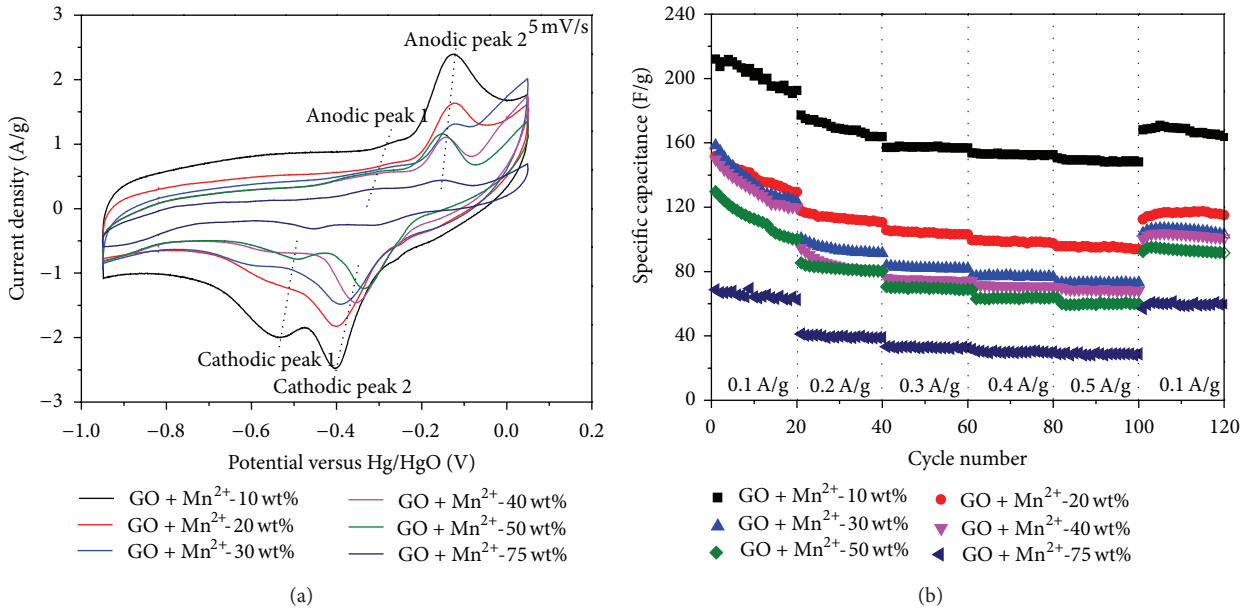

FIGURE 6: Electrochemical behaviors of GM composites in the 6 M KOH solution. (a) CV curves at 5 mV/s and (b) rate performance of GM composites prepared with different mass percent of Mn^{2+}/GO.

ensuring good electrical contracts between GS and Mn_3O_4 nanoparticles. Based on the TEM images (insetted in Figures 5(c) and 5(d)) of GM composites prepared with Mn^{2+}/GO mass percent of 50 : 50 and 10 : 90, respectively, EDS spectra (Figures 5(g) and 5(h)) present the only strong peak signals of manganese, carbon, and oxygen elements, components of the GM composite.

3.3. Electrochemical Performances. Figure 6(a) shows the CV curves of GM composites prepared with different mass percent of Mn^{2+}/GO. All curves have two pairs of redox peaks in the potential range from −0.95 to 0.05 V at a scan rate of 5 mV/s. This indicates that the pseudocapacitances can be obtained by the redox transitions of interfacial oxidation species at different oxidation states of Mn (7) and Mn (7) of GM composites. The mechanism may be explained with the following Faradaic reactions [46, 47]:

$$3\mathrm{Mn(OH)_2} + 2\mathrm{OH^{-1}} \leftrightarrows \mathrm{Mn_3O_4 \cdot 2H_2O} + 2\mathrm{e} + 2\mathrm{H_2O} \quad (1)$$

$$\mathrm{Mn_3O_4 \cdot 2H_2O} + \mathrm{OH^{-1}} \leftrightarrows 2\mathrm{MnOOH} + \mathrm{Mn(OH)_3} + \mathrm{e} \quad (2)$$

In these two equations, (1) accounts for the redox reactions at the anodic and cathodic peaks 1, while (2) is for the anodic and cathodic peaks 2. It should also be observed that the capacitive current responses increase with decreasing the Mn^{2+}/GO mass percent. The specific capacitances of GM composites prepared with Mn^{2+}/GO mass percent of 10 : 90, 20 : 80, 30 : 70, 40 : 60, 50 : 50, and 75 : 25 can be calculated using (3), where I is the voltammetric current (A), m is the mass of the active materials in electrode (g), ΔV is the potential window (V), and r is the scan rate (V/s). As a result, their values are 244.78, 174.04, 159.01, 142.89, 136.28, and 55.37 F/g, respectively,

$$C_{sp} = \frac{\int I(V)\, dV}{m \times \Delta V \times r}. \quad (3)$$

The rate performances (Figure 6(b)) of GM composites prepared with different mass percent of Mn^{2+}/GO have been studied by means of GCD technique. These electrodes are continued 20 cycles at each of the current densities (0.1, 0.2, 0.3, 0.4, and 0.5 A/g) and then brought back to 0.1 A/g in the reverse order to run another 20 cycles. It should be noted that the less $Mn(CH_3COO)_2 \cdot 4H_2O$ powder is added, the higher the specific capacitance of the as-prepared GM composite is. The result is consistent with that deduced from the CV tests.

Figure 6(b) shows that the specific capacitance of GM composite prepared with Mn^{2+}/GO mass percent of 10 : 90 is nearly three times higher than that of GM composite prepared with Mn^{2+}/GO mass percent of 75 : 25 at 0.1 A/g. The capacitance retention rates of GM composites prepared with Mn^{2+}/GO mass percent of 10 : 90, 20 : 80, 30 : 70, 40 : 60, 50 : 50, and 75 : 25 are 71.02%, 63.00%, 46.16%, 47.10%, 49.74%, and 41.82% at 0.5 A/g, respectively. The results illustrate that the decrease of Mn^{2+}/GO mass percent may help to enhance the capacity and rate performance of GM composite.

This is because GM composites can provide higher specific capacitance and display better rate capability mainly through fast and effective charge transfer in the electrode. Combined with the TEM images (Figures 5(c) and 5(d)) of GM composites, the Mn_3O_4 nanoparticles loaded on the surface of GS are found to agglomerate easily with an increase of the mass percent of Mn^{2+}/GO. The agglomeration of Mn_3O_4 nanoparticles greatly increases interparticle resistance of the electron pathways and hinders the interfacial

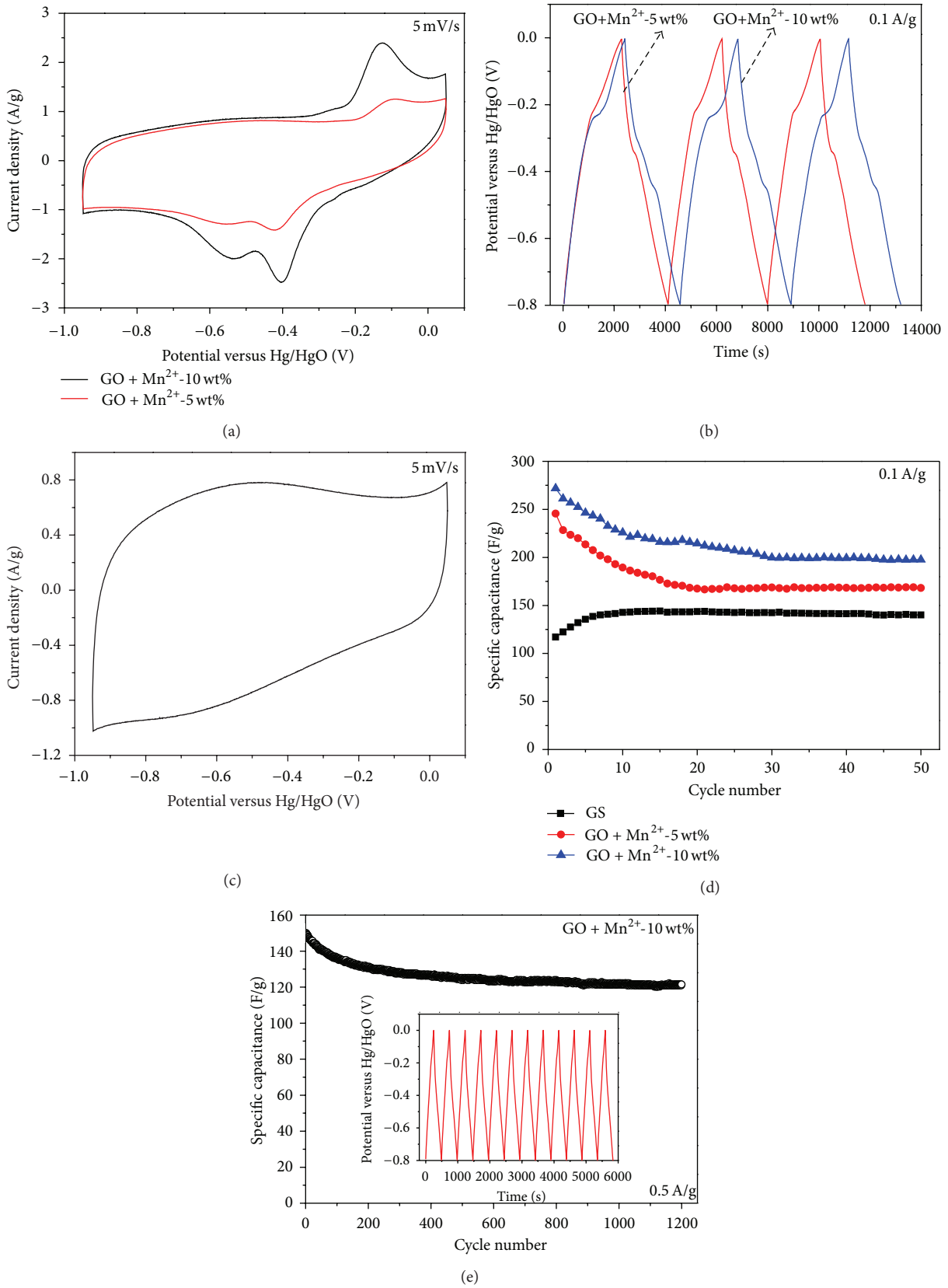

Figure 7: (a) CV curves and (b) GCD curves of GM composites prepared with Mn^{2+}/GO mass percent of 10 : 90 and 5 : 95, (c) CV curve of GS, (d) specific capacitance of GS and GM composites prepared with Mn^{2+}/GO mass percent of 10 : 90 and 5 : 95 versus cycle number at 0.1 A/g, and (e) specific capacitance of GM composite prepared with Mn^{2+}/GO mass percent of 10 : 90 versus cycle number at 0.5 A/g. The *inset* is the charge/discharge curves.

contact between Mn_3O_4 nanoparticles and GS, resulting in limited electrochemical utilization of Mn_3O_4. Hence, the GM composite prepared with Mn^{2+}/GO mass percent of 10 : 90 can exhibit the best electrochemical performance.

From the CV curves (Figure 7(a)) and GCD curves (Figure 7(b)) analysis, the specific capacitance obtained by GM composite prepared with Mn^{2+}/GO mass percent of 10 : 90 is higher than that by GM composite prepared with Mn^{2+}/GO mass percent of 5 : 95. Figure 7(c) shows the CV curve of GS obtained by solvothermal reduction of GO at 473 K, which is quasi-rectangular shape without obvious redox peaks, indicating the ideal capacitive behavior of GS. By (3) calculations, the specific capacitances of GM composites prepared with Mn^{2+}/GO mass percent of 10 : 90 and 5 : 95 and GS are 244.78, 179.74, and 139.45 F/g at 5 mV/s, respectively. Moreover, the specific capacitances of GM composites prepared with Mn^{2+}/GO mass percent of 10 : 90 and 5 : 95 and GS as the functions of cycle number are presented in Figure 7(d). It can be observed that the specific capacitance of GM composite prepared with Mn^{2+}/GO mass percent of 10 : 90 is the largest while the specific capacitance of GS is the least. This further indicates that the contribution of Mn_3O_4 electrochemical reactions to the total specific capacitance is predominant. GM composite prepared with Mn^{2+}/GO mass percent of 10 : 90 can provide more electroactive sites for redox reactions than that obtained by GM composite prepared with Mn^{2+}/GO mass percent of 5 : 95, so the optimal mass percent of Mn^{2+}/GO to produce the GM composite is 10 : 90.

Figure 7(e) shows the cycle stability of GM composite prepared with Mn^{2+}/GO mass percent of 10 : 90. It is seen that over 81% of the origin specific capacitance has been retained at 0.5 A/g after 1200 cycles, displaying the better long-term electrochemical stability. The reason is that adopting the optimal mass percent of Mn^{2+}/GO to prepare the GM composite prevents the agglomeration of Mn_3O_4 nanoparticles and the loss of electric contact between the Mn_3O_4 nanoparticles and GS. Meanwhile, Mn_3O_4 nanoparticles have been inserted into GS to avoid the exfoliation of Mn_3O_4 nanoparticles attributed to their volume expansions during cycling at a bigger current density.

4. Conclusion

We have developed a simple and "green" solvothermal method to produce the GM composites. The structure and composition of GM composites were investigated. The results indicated that the nanoparticles loaded GS had the tetragonal hausmannite structure of Mn_3O_4. TEM images of GM composites showed that Mn_3O_4 nanoparticles happened to agglomerate on the surface of GS with the increase of the mass percent of Mn^{2+}/GO. The electrochemical performances of these GM composites have been studied by CV and GCD. The results showed that GM composite prepared with the optimal mass percent of Mn^{2+}/GO (10 : 90) could provide a higher specific capacitance (~245 F/g) at 5 mV/s and the specific capacitance only decreased by 19% of the initial capacitance at 0.5 A/g after 1200 cycles. Hence, GM composite material is a promising candidate for SCs.

Conflict of Interests

The authors have declared that they have no conflict of interests.

Acknowledgments

This work was financially supported by the Natural Science Foundation of China (21076050) and Natural Science and Technology Support Program of China (2013BAE04B04).

References

[1] A. Burke, "Ultracapacitors: why, how, and where is the technology," *Journal of Power Sources*, vol. 91, no. 1, pp. 37–50, 2000.

[2] L. L. Zhang and X. S. Zhao, "Carbon-based materials as supercapacitor electrodes," *Chemical Society Reviews*, vol. 38, no. 9, pp. 2520–2531, 2009.

[3] B. E. Conway, V. Birss, and J. Wojtowicz, "The role and utilization of pseudocapacitance for energy storage by supercapacitors," *Journal of Power Sources*, vol. 66, no. 1-2, pp. 1–14, 1997.

[4] G. Wang, L. Zhang, and J. Zhang, "A review of electrode materials for electrochemical supercapacitors," *Chemical Society Reviews*, vol. 41, no. 2, pp. 797–828, 2012.

[5] J. P. Zheng, P. J. Cygan, and T. R. Jow, "Hydrous ruthenium oxide as an electrode material for electrochemical capacitors," *Journal of the Electrochemical Society*, vol. 142, no. 8, pp. 2699–2703, 1995.

[6] C.-C. Hu, Y.-H. Huang, and K.-H. Chang, "Annealing effects on the physicochemical characteristics of hydrous ruthenium and ruthenium-iridium oxides for electrochemical supercapacitors," *Journal of Power Sources*, vol. 108, no. 1-2, pp. 117–127, 2002.

[7] G. Zhu, H. J. Li, L. J. Deng, and Z. H. Liu, "Low-temperature synthesis of δ-MnO_2 with large surface area and its capacitance," *Materials Letters*, vol. 64, no. 6, pp. 1763–1765, 2010.

[8] D. P. Dubal, D. S. Dhawale, R. R. Salunkhe, V. J. Fulari, and C. D. Lokhande, "Chemical synthesis and characterization of Mn_3O_4 thin films for supercapacitor application," *Journal of Alloys and Compounds*, vol. 497, no. 1-2, pp. 166–170, 2010.

[9] T.-C. Liu, W. G. Pell, and B. E. Conway, "Stages in the development of thick cobalt oxide films exhibiting reversible redox behavior and pseudocapacitance," *Electrochimica Acta*, vol. 44, no. 17, pp. 2829–2842, 1999.

[10] C. Yuan, X. Zhang, L. Su, B. Gao, and L. Shen, "Facile synthesis and self-assembly of hierarchical porous NiO nano/micro spherical superstructures for high performance supercapacitors," *Journal of Materials Chemistry*, vol. 19, no. 1, pp. 5772–5777, 2009.

[11] M. Nakayama, A. Tanaka, Y. Sato, T. Tonosaki, and K. Ogura, "Electrodeposition of manganese and molybdenum mixed oxide thin films and their charge storage properties," *Langmuir*, vol. 21, no. 13, pp. 5907–5913, 2005.

[12] L. Li, Z. Guo, A. Du, and H. Liu, "Rapid microwave-assisted synthesis of Mn_3O_4-graphene nanocomposite and its lithium storage properties," *Journal of Materials Chemistry*, vol. 22, no. 8, pp. 3600–3605, 2012.

[13] Y. Huang, J. Liang, and Y. Chen, "An overview of the applications of graphene-based materials in supercapacitors," *Small*, vol. 8, no. 12, pp. 1805–1834, 2012.

[14] X. Cui, F. Hu, W. Wei, and W. Chen, "Dense and long carbon nanotube arrays decorated with Mn_3O_4 nanoparticles for electrodes of electrochemical supercapacitors," *Carbon*, vol. 49, no. 4, pp. 1225–1234, 2011.

[15] G. An, P. Yu, M. Xiao et al., "Low-temperature synthesis of Mn_3O_4 nanoparticles loaded on multi-walled carbon nanotubes and their application in electrochemical capacitors," *Nanotechnology*, vol. 19, no. 27, Article ID 275709, 2008.

[16] T. Zhou, S. Mo, S. Zhou, W. Zou, Y. Liu, and D. Yuan, "Mn_3O_4/worm-like mesoporous carbon synthesized via a microwave method for supercapacitors," *Journal of Materials Science*, vol. 46, no. 10, pp. 3337–3342, 2011.

[17] L.-L. Chen, X.-L. Wu, Y.-G. Guo, Q.-S. Kong, and Y.-Z. Xia, "Synthesis of nanostructured fibers consisting of carbon coated Mn_3O_4 nanoparticles and their application in electrochemical capacitors," *Journal of Nanoscience and Nanotechnology*, vol. 10, no. 12, pp. 8158–8163, 2010.

[18] K. Wang, X. Ma, Z. Zhang, M. Zheng, Z. Geng, and Z. Wang, "Indirect transformation of coordination-polymer particles into magnetic carbon-coated Mn_3O_4 (Mn_3O_4@C) nanowires for supercapacitor electrodes with good cycling performance," *Chemistry—A European Journal*, vol. 19, no. 22, pp. 7084–7089, 2013.

[19] K. S. Novoselov, A. K. Geim, S. V. Morozov et al., "Electric field in atomically thin carbon films," *Science*, vol. 306, no. 5696, pp. 666–669, 2004.

[20] J. Xia, F. Chen, J. Li, and N. Tao, "Measurement of the quantum capacitance of graphene," *Nature Nanotechnology*, vol. 4, no. 8, pp. 505–509, 2009.

[21] L. Wang, Y. Li, Z. Han et al., "Composite structure and properties of Mn_3O_4/graphene oxide and Mn_3O_4/graphene," *Journal of Materials Chemistry A*, vol. 1, no. 29, pp. 8385–8397, 2013.

[22] J. W. Lee, A. S. Hall, J.-D. Kim, and T. E. Mallouk, "A facile and template-free hydrothermal synthesis of Mn_3O_4 nanorods on graphene sheets for supercapacitor electrodes with long cycle stability," *Chemistry of Materials*, vol. 24, no. 6, pp. 1158–1164, 2012.

[23] Y. Wu, S. Liu, H. Wang, X. Wang, X. Zhang, and G. Jin, "A novel solvothermal synthesis of Mn_3O_4/graphene composites for supercapacitors," *Electrochimica Acta*, vol. 90, pp. 210–218, 2013.

[24] Y. Fan, X. Zhang, Y. Liu, Q. Cai, and J. Zhang, "One-pot hydrothermal synthesis of Mn_3O_4/graphene nanocomposite for supercapacitors," *Materials Letters*, vol. 95, pp. 153–156, 2013.

[25] G. S. Gund, D. P. Dubal, B. H. Patil, S. S. Shinde, and C. D. Lokhande, "Enhanced activity of chemically synthesized hybrid graphene oxide/Mn_3O_4 composite for high performance supercapacitors," *Electrochimica Acta*, vol. 92, pp. 205–215, 2013.

[26] Y. C. Liu, D. W. He, H. P. Wu, and J. H. Duan, "Graphene and nanostructured Mn_3O_4 composites for supercapacitors," *Integrated Ferroelectrics*, vol. 144, no. 1, pp. 118–126, 2013.

[27] J. Qu, F. Gao, Q. Zhou et al., "Highly atom-economic synthesis of graphene/Mn_3O_4 hybrid composites for electrochemical supercapacitors," *Nanoscale*, vol. 5, no. 7, pp. 2999–3005, 2013.

[28] C.-L. Liu, K.-H. Chang, C.-C. Hu, and W.-C. Wen, "Microwave-assisted hydrothermal synthesis of Mn_3O_4/reduced graphene oxide composites for high power supercapacitors," *Journal of Power Sources*, vol. 217, pp. 184–192, 2012.

[29] X. Zhang, X. Sun, Y. Chen, D. Zhang, and Y. Ma, "One-step solvothermal synthesis of graphene/Mn_3O_4 nanocomposites and their electrochemical properties for supercapacitors," *Materials Letters*, vol. 68, pp. 336–339, 2012.

[30] Z. Weixin, W. Cheng, Z. Xiaoming, X. Yi, and Q. Yitai, "Low temperature synthesis of nanocrystalline Mn_3O_4 by a solvothermal method," *Solid State Ionics*, vol. 117, no. 3-4, pp. 331–335, 1999.

[31] Y. C. Zhang, T. Qiao, and X. Ya Hu, "Preparation of Mn_3O_4 nanocrystallites by low-temperature solvothermal treatment of γ-MnOOH nanowires," *Journal of Solid State Chemistry*, vol. 177, no. 11, pp. 4093–4097, 2004.

[32] A. Vázquez-Olmos, R. Redón, G. Rodríguez-Gattorno et al., "One-step synthesis of Mn_3O_4 nanoparticles: structural and magnetic study," *Journal of Colloid and Interface Science*, vol. 291, no. 1, pp. 175–180, 2005.

[33] C. Nethravathi and M. Rajamathi, "Chemically modified graphene sheets produced by the solvothermal reduction of colloidal dispersions of graphite oxide," *Carbon*, vol. 46, no. 14, pp. 1994–1998, 2008.

[34] W. S. Hummers Jr. and R. E. Offeman, "Preparation of graphitic oxide," *Journal of the American Chemical Society*, vol. 80, no. 6, article 1339, 1958.

[35] Y. Xu, K. Sheng, C. Li, and G. Shi, "Self-assembled graphene hydrogel via a one-step hydrothermal process," *ACS Nano*, vol. 4, no. 7, pp. 4324–4330, 2010.

[36] D. P. Dubal, D. S. Dhawale, R. R. Salunkhe, S. M. Pawar, V. J. Fulari, and C. D. Lokhande, "A novel chemical synthesis of interlocked cubes of hausmannite Mn_3O_4 thin films for supercapacitor application," *Journal of Alloys and Compounds*, vol. 484, no. 1-2, pp. 218–221, 2009.

[37] J. Zhang, H. Yang, G. Shen, P. Cheng, J. Zhang, and S. Guo, "Reduction of graphene oxide vial-ascorbic acid," *Chemical Communications*, vol. 46, no. 7, pp. 1112–1114, 2010.

[38] C. D. Wagner, G. E. Muilenberg, L. E. Davis, and J. F. Moulder, *Handbook of X-Ray Photo Electron Spectroscopy: A Reference Book of Standard Data for Use in X-Ray Photo Electron Spectroscopy*, Physical Electronics Division, Perkin Elmer, Eden Prairie, Minn, USA, 1979.

[39] A. Moses Ezhil Raj, S. G. Victoria, V. B. Jothy et al., "XRD and XPS characterization of mixed valence Mn_3O_4 hausmannite thin films prepared by chemical spray pyrolysis technique," *Applied Surface Science*, vol. 256, no. 9, pp. 2920–2926, 2010.

[40] C. M. Julien, M. Massot, and C. Poinsignon, "Lattice vibrations of manganese oxides: part I. Periodic structures," *Spectrochimica Acta—Part A: Molecular and Biomolecular Spectroscopy*, vol. 60, no. 3, pp. 689–700, 2004.

[41] L. Li, K. H. Seng, H. Liu, I. P. Nevirkovets, and Z. Guo, "Synthesis of Mn_3O_4-anchored graphene sheet nanocomposites via a facile, fast microwave hydrothermal method and their supercapacitive behavior," *Electrochimica Acta*, vol. 87, pp. 801–808, 2013.

[42] Z. J. Li, B. C. Yang, S. R. Zhang, and C. M. Zhao, "Graphene oxide with improved electrical conductivity for supercapacitor electrodes," *Applied Surface Science*, vol. 258, no. 8, pp. 3726–3731, 2012.

[43] Y. Matsuo, K. Iwasa, Y. Sugie, A. Mineshige, and H. Usami, "Preparation of carbon-based transparent and conductive thin films by pyrolysis of silylated graphite oxides," *Carbon*, vol. 48, no. 14, pp. 4009–4014, 2010.

[44] S. Stankovich, D. A. Dikin, R. D. Piner et al., "Synthesis of graphene-based nanosheets via chemical reduction of exfoliated graphite oxide," *Carbon*, vol. 45, no. 7, pp. 1558–1565, 2007.

[45] K. Ku, B. Kim, H. Chung, and W. Kim, "Characterization of graphene-based supercapacitors fabricated on Al foils using Au or Pd thin films as interlayers," *Synthetic Metals*, vol. 160, no. 23-24, pp. 2613–2617, 2010.

[46] B. Messaoudi, S. Joiret, M. Keddam, and H. Takenouti, "Anodic behaviour of manganese in alkaline medium," *Electrochimica Acta*, vol. 46, no. 16, pp. 2487–2498, 2001.

[47] L. Zhu, S. Zhang, Y. Cui, H. Song, and X. Chen, "One step synthesis and capacitive performance of graphene nanosheets/Mn_3O_4 composite," *Electrochimica Acta*, vol. 89, pp. 18–23, 2013.